Plasma Medicine, 2(1-3): 151–168 (2012)

Optical Emission Spectroscopy as a Tool for Characterization of Technical Plasmas in Medical Applications

Peter Awakowicz, Sabrina Baldus, Katharina Stapelmann, Max Engelhardt, Nikita Bibinov & Benjamin Denis

[1]Department of Electrical Engineering and Plasma Technology, Ruhr-Universität Bochum, Bochum, Germany

*Address all correspondence to: Benjamin Denis; Institute for Electrical Engineering and Plasma Technology (AEPT) Ruhr-Universität Bochum, 44780 Bochum, Germany; denis@aept.ruhr-uni-bochum.de

ABSTRACT: Understanding the interactions of technical plasma discharges with biological systems is a key aspect to developing and optimizing plasma devices for use in medical practice. In this article, the characterization of 3 different plasma devices with absolutely and relatively calibrated optical emission spectroscopy is presented. Two low-pressure setups are described: a double inductively coupled plasma that serves as laboratory setup for basic research of sterilization of spores and germs and a very high frequency capacitively coupled plasma designed to meet commercial needs. An atmospheric pressure dielectric barrier discharge is designed for wound and skin treatment. Sterilization tests for each setup demonstrate the capability to inactivate bacteria and bacterial spores efficiently. In case of the double inductively coupled plasma, wavelength-dependent photo sterilization efficiency is investigated. As a result, *Aspergillus brasiliensis* spores are efficiently inactivated by irradiation below 235 nm, whereas *Bacillus atrophaeus* spores are sensitive to irradiation between 235 and 300 nm. The very high frequency capacitively coupled plasma demonstrates a reduction greater than log 6 of *B. Atrophaeus* endospores in a process challenge device, a metal box with 3 small slits (3 mm). With direct DBD treatment, a full inactivation of *Escherichia coli* is achieved within 10 seconds of treatment time. From measurements, data can be extracted only at certain positions. Simulations deliver spatially resolved data from whole-discharge volume.

KEY WORDS: OES, plasma sterilization, ICP, CCP, DBD, HPEM

I. INTRODUCTION

The application of technical plasma for biological and medical purposes has grown over the past few decades.[1] Especially atmospheric pressure plasmas gained research interest, offering a wide range of possible applications, for example, in wound treatment or skin treatment in general. Low-pressure plasmas for sterilization and decontamination of various surfaces are already in use or show promise for use in the future.

Low-pressure plasma treatment offers certain advantages compared to other established sterilization methods, such as avoiding toxic chemical agents or the possibility of treating sensitive and thermolabile materials. Different low-pressure plasma setups have been investigated for many years for sterilization purposes,[2–5] they offer the opportunity to inactivate, for example, bacteria, bacterial spores, fungi, as well as to remove biologi-

1947-5764/12/$35.00

cal material from surfaces of, for example, proteins and prions.[6–8] The first low-pressure plasma reactor for sterilization was recently presented by the pharmaceutical industry.[9]

Atmospheric pressure plasmas are still far from actually being applied in medical practice and are currently objects of research. There is a wide variety of different discharge types, such as dielectric barrier discharges (DBDs), plasma jets, and hollow cathodes, aiming to disinfect skin and wounds, support wound healing, accelerate blood coagulation, reduce cancer cells or have positive cosmetic effects.[10–18] Those plasma sources can be used outside or even inside the human body.

To understand the different plasma processes and the interaction of technical plasmas with biological systems, detailed knowledge of the plasma itself is indispensable. Plasma characterization is the key to understanding and optimizing plasma for sterilization, disinfection, and decontamination and for the application of therapy in humans. Absolutely calibrated optical emission spectroscopy (OES) and plasma simulations offer deep insight into plasma processes and the interaction of plasmas and cells. These diagnostic methods complement each other and provide information concerning photon fluxes on the surfaces of treated objects and can be used to optimize of sterilization efficiency.

II. MATERIALS AND METHODS

A. Plasma Setups

Two different low-pressure regime setups and one atmospheric pressure setup for sterilization and disinfection are presented in this article, namely a double inductively coupled plasma (DICP), a very high frequency capacitively coupled plasma (VHF-CCP), and a dielectric barrier discharge DBD that is operational under atmospheric pressure conditions. The DICP serves as a laboratory setup for basic research, whereas the VHF-CCP has its focus on commercial application. The DBD aims to work during skin contact for wound healing and wound disinfection.

1. DICP Setup

A detailed description of the reactor and a plasma characterization in different argon mixtures has already been presented.[19] The DICP consists of a stainless steel cylinder enclosed with quartz windows. Coils behind these windows are driven with a radiofrequency (RF) current at 13.56 MHz under inductively coupled plasma excitation with a maximum power output of 5000 W. It is operated in a low pressure plasma regime with a volume of 0.025 m^3. Different gases (argon, nitrogen, oxygen) and their mixtures enter the reactor through a gas shower. The working pressure is adjustable between 5 and 20 Pa.

This discharge is characterized by OES and a Langmuir probe. Two different OES measuring positions are used: one near the active plasma zone and another located at the middle height of the reactor, far from active plasma zones. The Langmuir probe is attached at the middle position. To mimic a sterilization process, a cylindrical glass object is placed in the middle of the DICP as a sterilization payload.

2. VHF-CCP Setup

The VHF-CCP plasma reactor is a low-pressure, capacitively coupled plasma source. The discharge chamber is composed of polyether ether ketone, a high-performance plastic, and shaped like a drawer, with an inner size of 0.32 × 0.22 m. The 2 electrodes are adapted to the same area as the chamber, with a distance between the grounded and driven electrodes of 0.08 m. Attached to the grounded electrode is a rotary vane pump (Trivac D65B; Oerlikon Leybold Vacuum, Cologne, Germany). A gas inlet system through a gas shower inside the grounded electrode allows a homogeneous discharge. The gas inlet system comprises mass flow controllers (MFC Type 1179; MKS Instruments, Munich, Germany) for argon, nitrogen, oxygen and hydrogen, with a constant total gas flow of 20 sccm. The pressure is controlled by a butterfly valve (Butterfly valve control system Series 612; VAT Germany, Grasbrunn/Munich, Germany), adjustable between 5 and 25 Pa. The VHF-CCP is driven by an RF source, operating at a frequency of 81.36 MHz with a maximum power output of 500 W. It is matched to the discharge through a variable matching network in T-type configuration (both from Aurion, Seligenstadt, Germany). This setup derives the advantages from CCP, that is, a high electric field for a better penetration of small lumen, combined with a higher electron density and lower ion energy due to the high frequency used. The capability to enter small lumen provided by this setup is proofed by a so-called process challenging device (PCD; see Fig. 1).

3. DBD Operating on Human Skin

The DBD used at our institute comprises a single aluminium oxide-coated copper electrode with a 10 mm total diameter. Every object with high capacitance (such as human tissue) serves as a counter electrode. Because plasma can be ignited directly on the surface of the human body, it is a so-called direct treatment. The discharge is ignited in

FIG. 1: A process challenging device: a metal box with 3 slits of 0.3 mm width.

the gap between the electrode and tissue in ambient air as process gas. A high-voltage supply with a peak amplitude of –13 kV and an oscillation frequency of 100 kHz is modulated with a frequency of 300 Hz. This setup leads to current peaks with short durations (10–20 ns), which are essential to keeping the mean power low and the treatment pain-free for the patient.[20–23]

The DBD is characterized using OES, current-voltage measurements, numerical simulation, and microphotography. All these methods complement each other to allow determination of gas temperature and averaged plasma parameters, such as electron density and electron velocity distribution function in the active plasma volume.

B. Microbiological Analysis

1. Spores and Endospores

For the evaluation and validation of low-pressure plasmas for sterilization and decontamination of medical instruments or implants, (endo)spores play a major role. Since (endo)spores are more resistant than vegetative cells, only sterilization tests with (endo) spores are carried out in DICP and VHF-CCP. Therefore, spores of relevance for sterilization devices are chosen to perform sterilization tests, for example, *Bacillus atrophaeus*, which serves as an bioindicator for gas sterilization. Furthermore, spores of *Aspergillus brasiliensis* were chosen, because they are known to be resistant against ultraviolet (UV) radiation because of their pigmentation.[4,24]

The microbiological samples for the spore and endospore experiments were prepared and analyzed by the Fraunhofer Institute for Process Engineering and Packaging in Freising, Germany. Germs diluted in aqueous solution are sprayed on 1 cm^2 glass slides. Endospores of *B. atrophaeus* ATCC 51189 and spores of *A. brasiliensis* ATCC 16404 were used; 10^6 and 10^7 colony forming units (CFUs), respectively, were recovered from untreated samples. Scanning electron microscopy images show a monolayer of (endo) spores on the glass slides. The samples were treated in the DICP or VHF-CCP reactor. After treatment the samples were washed with Ringer-Tween solution. Dilution series were made and pipetted on culture medium, and the resulting CFUs were counted. Muranyi *et al*.[25–27] described the process in more detail. The CFUs after treatment were compared to the CFUs of untreated samples; a log-reduction R is given as:

$$R = \log \frac{CFU_{\text{untreated}}}{CFU_{\text{treated}}}. \tag{1}$$

2. Vegetative Cells

For wound disinfection, harmless strains of gram-negative bacterium *Escherichia coli* were used. These bacteria are part of the normal flora of the intestinal tract of mammals, where they are capable of preventing pathogen growth and producing vitamin K. Pathogenic strains can cause foodborne illnesses, gastroenteritis, urinary tract infections, or neonatal meningitis.

For treatment, *E. coli* DSM 18039 was diluted in water, then 5 µL were sprayed on a glass slide and dried, leading to a monolayer of *E. coli* bacteria. The resulting CFUs were counted and compared to the CFUs after DBD plasma treatment as it is described above.

C. Plasma Diagnostics

1. Optical Emission Spectroscopy

Three optical spectrometers were applied: an echelle spectrometer (ESA 3000; LLA Instruments) with an intensified charge coupled device sensor, a grating spectrometer (QE65000; Ocean Optics) with a charge coupled device sensor, and a UV/Vacuum UV (VUV) grating monochromator (Jobin-Yvon AS50) equipped with a solar-blind photomultiplier. The echelle spectrometer has a spectral resolution of 0.015–0.06 nm in the wavelength range of 200–800 nm. The QE65000 offers a spectral resolution of 1.3 nm in the wavelength range of 200–975 nm. The UV/VUV spectrometer setup measures in the spectral range of 115–300 nm, with a spectral resolution of 0.3 nm. These spectrometers are relatively and absolutely calibrated, as described elsewhere.[28,29]

The echelle spectrometer is able to resolve rotational structures of molecular transitions. Gas temperature in the active plasma volume is determined using the well-known spectrum of nitrogen molecules and numerical simulation of nitrogen molecule spectra at various gas temperatures. It is assumed that the lifetime of nitrogen molecules in the ground state is sufficient for relaxation to equilibrium between rotational and translational degrees of freedom, that is rotational and translational temperatures are equal. Since electron impact excitation changes the momentum of nitrogen molecules only marginally, distribution of the rotational energy-level population in excited states is equal to the ground state distribution. Rotational temperatures determined from photoemission of nitrogen molecules mainly excited by electron impact are similar or even equal to gas temperature. To determine gas temperature, the "second positive" system of neutral nitrogen emission N_2(C–B, 0–0) was used.

The QE65000 is suitable for measurement of broad-band emissions (e.g., hydrogen continuum), because of its low spectral resolution. The optical fibers of UV/Visible spectrometers are equipped with a diaphragm to confine the acceptance angle. To determine the intensity of photon emission (in photons per seconds, cubic centimetres and nanometres), the measured emission spectrum, the absolute spectral efficiency of the applied spectrometer, and the corresponding plasma volume observed by the spectrometer were used.

The VUV monochromator can only be attached to the DICP for technical reasons. There, a spectrum in the wavelength range of 115–240 nm was measured and combined with the spectrum measured with the echelle spectrometer in the wavelength range of 200–800 nm. With this whole spectrum, the UV/VUV sensitivity of (endo) spores was determined.

2. Determination of Electron Energy Distribution Functions

The methods for determining electron energy distribution functions (EEDFs) differ under considered plasma conditions. In low-pressure DICP, the EEDF determination is based on a "two-temperature" assumption. Both parts of the distribution are assumed to be Maxwellian. The low-energy part of the EEDF, below 10 eV, is measured by a Langmuir probe system (APS 3 probe system[9]). The highly energetic tail is determined by OES with the echelle spectrometer. For that purpose, a small amount of nitrogen is admixed with the process gas. The amount of nitrogen is adjusted in a manner that enables detection of specific nitrogen molecular bands without altering the plasma conditions. This is controlled by checking the working gas photoemission. To determine the EEDF, a neutral and an ion molecular band, namely nitrogen gas (C-B, 0-0, $\lambda = 337.1$ nm) and nitrogen ion N-2^+ (B-X, 0-0, $\lambda = 391.4$ nm), are evaluated. The corresponding energy levels are populated by direct electron impact from $N_2(X)$ or stepwise excitation via the metastable state, $N_2(A)$, or ion ground state, $N_2^+(X)$. Excitation of N_2(C-B) photoemission by collisions with argon metastable, $Ar(^3P_{0,2})$, are also taken into account for the DICP setup. The quotient of the intensities of these 2 molecular bands provides the electron temperature T_e under assumption of a Maxwellian EEDF. Absolute band intensities subsequently yield the electron density n_e. A more detailed discussion of this method can be found elsewhere.[30,31] The EEDFs measured by Langmuir probe and determined by OES were compared and good agreement was found in the overlapping region of the 2 methods.

The two-temperature approach can be applied only to the DICP setup because the APS3 Langmuir probe system can not be attached to the VHF-CCP. Therefore, the same OES method as described above was used for the whole energy range of the EEDF, assuming a single Maxwellian distribution.

At atmospheric pressure the EEDF differs from maxwellian distribution because of inelastic collisions of oxygen and nitrogen molecules with electrons. Therefore the EEDF was determined using numerical simulation and OES. EEDF under DBD plasma conditions was determined by nitrogen molecular photoemission, under the assumption of direct excitation from the ground state of the nitrogen molecule $N_2(X)$. Validity of this assumption under DBD conditions was verified by Keller *et al*.[20] The ratio of the nitrogen bands N_2(C-B) and N_2^+(B-X) was calculated from the measured spectrum. The Boltzmann equation was solved numerically in local approximation for varied electric fields. Comparison of measurement results and simulation provided a distribution function determined from the best fit. This process was previously described in detail.[32]

3. Simulation of DICP

To obtain photon fluxes on all sides of a 3-dimensional object, a simulation of the laboratory DICP setup was performed using the Hybrid Plasma Equipment Model (HPEM) developed by Kushner.[33] HPEM is a hybrid code software, meaning that different species can be addressed with different methods. Electrons, which have a high velocity

and therefore need a high temporal resolution, are simulated with a kinetic approach; furthermore, this also allows for the calculation of non-Maxwellian distribution functions. This allows accurate calculation in a very short time, however, it also significantly increases the calculation time. Neutral and ionized species have notably lower velocities, so time scales are much longer and a fluid-dynamic approach is sufficient. Hence, calculation times for heavy species are much shorter. This hybrid approach delivers accurate results for all species while keeping the calculation time as low as possible. The DICP reactor geometry has to be reproduced in the HPEM, which is possible without any simplifications, including the dual coils and the cylindrical object that is placed within the discharge to mimic a process with an actual sterilization payload. All external parameters of the discharge, such as the applied RF signal and gas pressure, are set to values similar to experimental parameters.

As results, the simulation gives 2-dimensional, spatially resolved profiles of species, densities and values such as electron temperature or plasma potential. Furthermore, the temporal evolution of species toward steady-state solution can be observed. The intensity of photoemission is calculated in the frame of the corona model to:

$$I_{pk} = n_1 n_e k_{exc}(T_e), \tag{2}$$

where n_1 is the density of species in the ground state, n_e is the electron density, and k_{exc} is the rate coefficient for excitation from ground level, which is strongly dependent on the electron temperature.

III. RESULTS AND DISCUSSION

A. DICP

To have a closer look at the relative sterilization efficiency of UV/VUV radiation, different filter experiments were performed. Spores were sprayed in a 1 cm^2 square on glass slides and covered with different cut-off filters: magnesium fluoride (115 nm) and 2 glasses (235 and 300 nm). The filters were separated from the glass slides by glass rings. The samples were treated in the DICP in argon/nitrogen/oxygen (100:4:1 sccm) at 10 Pa and 750 W for 60 seconds. This plasma condition was chosen so that a similar amount of photons in each spectral interval (115–235, 235–300 and 300–450 nm) reached the sample. The spores were recovered and counted as described earlier. Further description of the procedure and the spectrum of the used plasma can be found elsewhere.[9,34] Fig. 2 shows the relative sterilization efficiency of *A. brasiliensis* and *B. atrophaeus*. For this, the log-reduction *R* was divided by the number of photons reaching the samples; the highest value is normalized to 1. The result shows that *B. atrophaeus* endospores are sensitive to radiation in the spectral range of 235–300 nm; in contrast, *A. brasiliensis* spores are much less sensitive to radiation above 235 nm. These spores are more sensitive to radiation in a spectral range of 115–235 nm. This result encourages the building of a fast sterilization reactor with high UV/VUV emission.

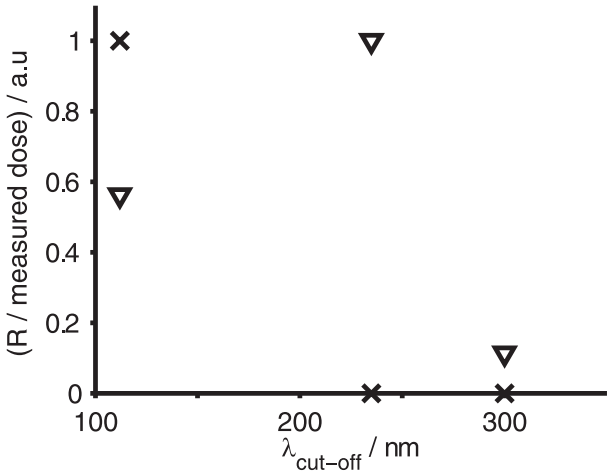

FIG. 2: Relative sterilization efficiency of *Bacillus atrophaeus* endospores (▽) and *Aspergillus brasiliensis* (X) spores.

B. VHF-CCP

In order to find efficient sterilization conditions, hydrogen, oxygen, and a mixture of both were investigated as process gases for plasma sterilization. At first, UV/VUV dose of the aforementioned process gases is investigated, since UV/VUV radiation is known to be one of the most efficient sterilization agents in the initial stage of plasma treatment[35]. Granted that, the discharge can be tuned to achieve efficient sterilization. A hydrogen discharge is known to emit a high quantity of photons in the UVC and UV/VUV range, among others, because of the hydrogen continuum H_2(a-b, λ = 158–350 nm). The emission spectrum obtained by the measurements with the QE65000 spectrometer starts at a wavelength of 200 nm. As shown previously, the radiation in the spectral range of 200–280 nm contributes only 13% of the total photons emitted in the UV/VUV range.[9] Since the characteristics of this continuum are well known, the band from 158 to 200 nm can be fitted to the measured spectrum. With a hydrogen discharge (20 sccm H_2, 5 Pa, 400 W), a total UV radiation of E_{tot} = 13.59 J m^{-2} s^{-1} (see Table 1) is reached, with E_{UVC} = 6.76 J m^{-2} s^{-1} in the most efficient UVC range, and E_{VUV} = 10.56 J m^{-2} s^{-1} considering the H_2(a-b) continuum in the VUV range. In comparison, pure oxygen discharge has a total UV dose of E_{tot} = 7.67 J m^{-2} s^{-1}, with E_{UVC} = 3.44 J m^{-2} s^{-1} in the UVC range. However, oxygen offers a high amount of reactive species, so it should be considered for removal of biological material because atomic oxygen is known as a good etching agent. In addition, the high number of radicals causes oxidative stress in cells. For plasma sterilization it is important to design the discharge to fit the application. If only inactivation of bacteria and bacterial spores is desired, a hydrogen discharge is most efficient. If there is a need to remove bacteria, bacterial endospores, and proteinaceous material, a gas mixture with oxygen, or a pure oxygen discharge, might be the most efficient.

TABLE 1. Ultraviolet (UV) Dose for the VHF-CCP Reactor

	UVA (315–380 nm)	UVB (280–315 nm)	UVC (200–280 nm)	VUVC (160–280 nm)	Total UV (200–380 nm)	Total UV, including VUV (160–380 nm)
H_2 (20 sccm)	1.67	1.28	6.79	10.56	9.78	13.59
H_2/O_2 (10/10 sccm)	1.59	1.74	3.93	5.12	7.3	8.48
O_2 (20 sccm)	1.9	2.24	3.44	3.97	7.67	8.19

Data is shown as J m^{-2} s^{-1}

To mimic a worst-case situation for plasma sterilization, a PCD is designed, consisting of a metal box with 3 small slits on top, as depicted in Fig. 1. The slits have a width of 0.3 mm. Glass slides are contaminated with *B. atrophaeus* ATCC 51189, as described earlier. The glass slides are placed inside the metal box. Afterward, the PCD is placed inside the process chamber and treated for 8, 16, 32, 64, 128, and 256 seconds with hydrogen plasma.

In Fig. 3 the results of the sterilization tests with the process challenging device are presented. The diagram shows the logarithmic reduction of *B. atrophaeus* spores treated

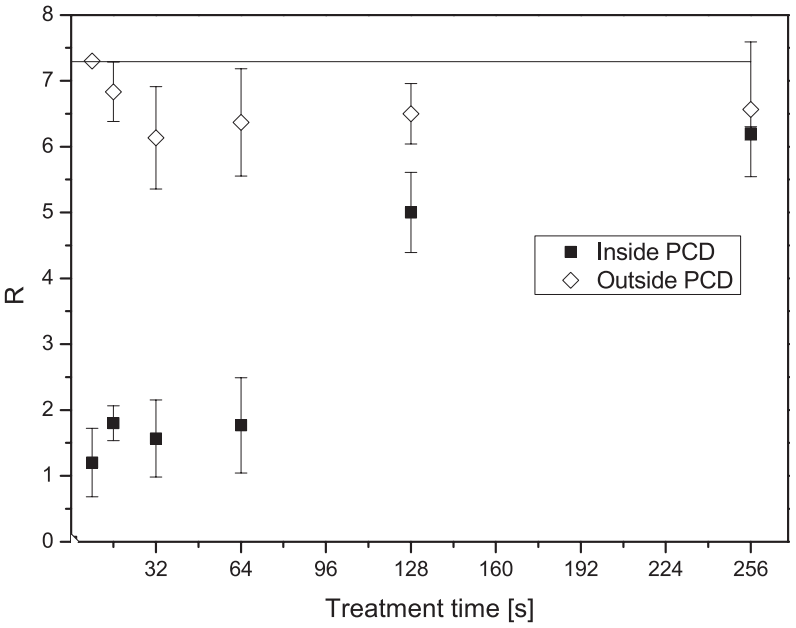

FIG. 3: Logarithmic reduction of *Bacillus atrophaeus* spores, placed inside a process challenging device (PCD) (black squares) and in comparison placed outside the PCD (white diamonds).

with hydrogen plasma at a pressure of 5 Pa and a power of 400 W. The black squares show the results for reduction inside the PCD, whereas the white squares show the results for samples placed outside the PCD, thus treated directly. While sterilization of directly treated *B. atrophaeus* spores happens instantaneously, sterilization inside the PCD takes longer. However, after around 4 minutes of plasma treatment, a reduction of $R = 6$ is achieved inside the PCD. The presented results demonstrate that sterilization with the VHF-CCP inside a PCD is possible. To optimize the plasma device for commercial use, it is necessary to tune the discharge to achieve fast and sufficient sterilization. With a pure hydrogen discharge, a high amount of UV/VUV radiation is available for fast sterilization. A pure oxygen discharge provides a high number of reactive species. A combination of both can lead to fast inactivation and removal of endospores and other biological material.

C. DBD Disinfection Purposes

E. coli cells sprayed on glass slides were treated with an atmospheric DBD. Treatment time varied while distance between the driven electrode and the sample was kept constant at 1 mm. *E. coli* bacteria were reduced after treatment for treatment times up to 10 seconds, shown in Fig. 4. After that time, no CFUs were recovered from plasma-treated glass slides; thus full cell inactivation was achieved. During this short treatment time, the inactivation of *E. coli* is mainly caused by UV radiation, considering that *E. coli* is known to be easily inactivated by UV light.

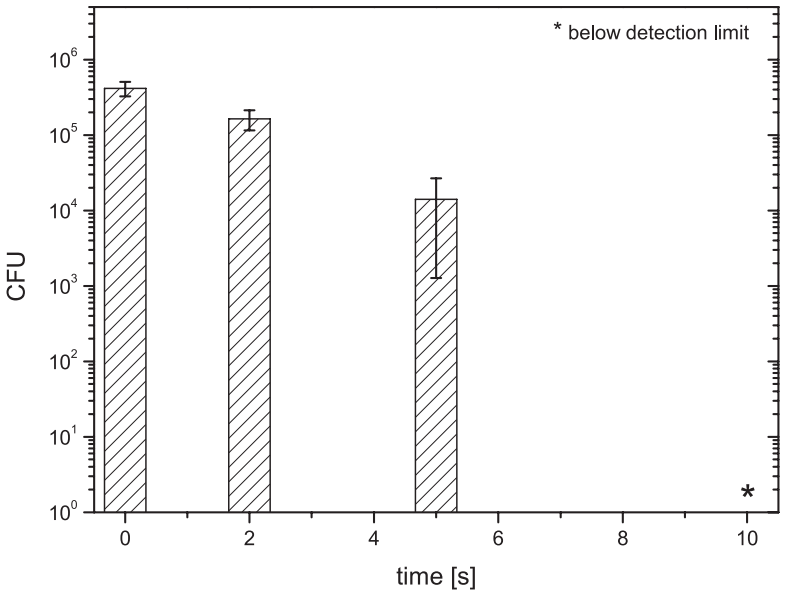

FIG. 4: Reduction of an *Escherichia coli* monolayer after dielectric barrier discharge treatment. CFU, colony-forming unit.

UV photoemission is measured in the range of 200–380 nm using the QE65000 spectrometer. Spectrum was absolutely calibrated as depicted in Fig. 5. Accordingly, the total photo energy emitted in the UV range was calculated to $E_{tot} = 0.155$ J m^{-2} s^{-1}, which is low in comparison to usual doses used in UV therapy. Most energy accounts for the UVA range (315–380 nm) $E_{UVA} = 0.099$ J m^{-2} s^{-1}, whereas photons in the UVB range (280–315 nm) only have $E_{UVB} = 0.017$ J m^{-2} s^{-1}. The least irradiation is measured in the UVC range (200–315 nm) $E_{UVC} = 0.004$ J m^{-2} s^{-1}.

It is obvious that a monolayer of *E. coli* bacteria can easily be inactivated by DBD treatment in short times. Since the DBD used in this investigation was designed with application in dermatology in mind, the disinfection of infected, chronic wounds is one important aspect. The ability to inactivate bacteria quickly leads to a relatively short treatment time of the infected wound. Because the interactions between plasma and human skin are not fully understood yet, a short treatment time is recommended to minimize possible negative effects for the patient. Knowledge of disinfection behavior of the DBD under different treatment conditions is significant and helpful since wounds, especially chronic wounds, are complex systems. Therefore, the effect on bacteria treated in liquid will be one of the aspects of further investigations. Furthermore, skin samples will be treated to determine interactions between skin and plasma.

D. EEDFs

In Fig. 6, electron energy distribution functions of 2 low-pressure setups, as well as EEDFs of atmospheric pressure DBDs are shown. The dashed line shows EEDFs of

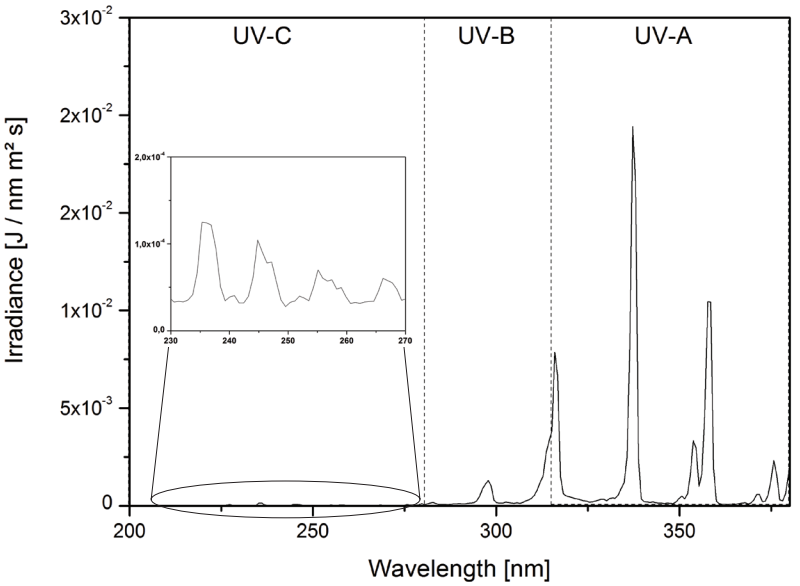

FIG. 5: Measured ultraviolet (UV) emission spectrum of dielectric barrier discharges.

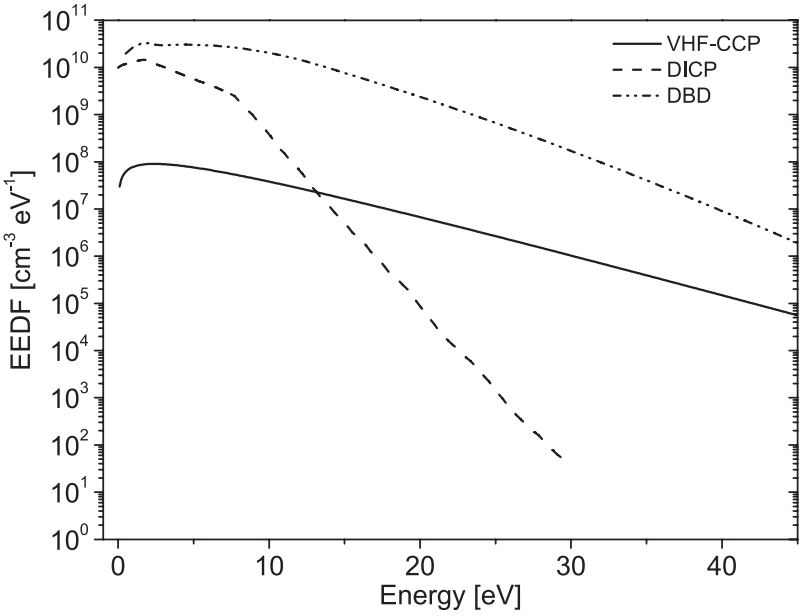

FIG. 6: Electron energy distribution functions (EEDFs) of very high frequency capacitively coupled plasma (VHF-CCP) (solid line), double inductively coupled plasma (DICP) (dashed line) and dielectric barrier discharge (DBD) (dotted and dashed line).

DICP, which exhibits an electron density two orders of magnitude higher. However, in the high-energy range above $E = 13$ eV, which is most important for excitation of UV and VUV radiation, the VHF-CCP (solid line) delivers a larger amount of electrons. This results in a higher production rate of UV/VUV photons and hence a higher intensity. The bend in the EEDF of the DICP setup around $E = 10$ eV can be clearly seen; this is caused by the 2-temperature approach of EEDF determination. The dot-and-dashed line shows EEDFs of DBD; its shape is typical for an atmospheric pressure plasma. The DBD device is operated in homogeneous mode.

E. Simulation of DICP

To produce homogeneous and intense radiation in the UV/VUV range, a hydrogen discharge is applied. Simulation is used to give insight into the homogeneity of UV irradiation on a 3-dimensional object. Only if irradiation on a payload object is uniform and sufficiently intense will sterilization results for the whole surface of the object be useful in applications. With OES measurement, some selected positions can be checked and used to verify simulation. From species densities and electron temperature, photoemission within plasma volume was calculated and compared with the measured one.

All measured data was collected by an echelle spectrometer connected to the discharge vessel with an optical fiber that was placed in front of a windowed flange. A cy-

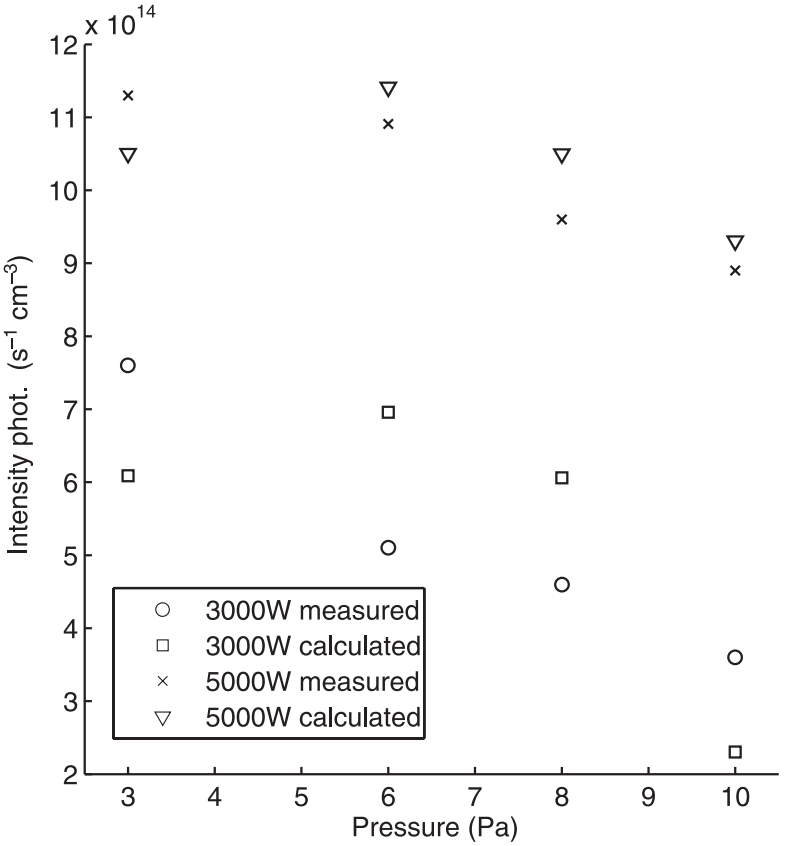

FIG. 7: Measured and calculated photon intensity in the active plasma region.

lindrical glass object was placed within the discharge to simulate a process with an actual sterilization payload. Fig. 7 shows measured and calculated photon intensities in the actively heated plasma zone close to the coil. Values are in good agreement to each other, especially for 5000-W accuracy, which is very good. Lower pressure leads to higher intensities, as does higher power input. It can be observed that the pressure that yields the highest intensity is calculated to be between 3 and 6 Pa. In measurements, 3 Pa still leads to a higher intensity. For 5000 W, measured intensity shows a weaker increase toward 3 Pa, which could indicate a maximum around this region.

A second measurement position is located at h = 10 cm, far from active plasma zones. Fig. 8 shows intensities measured within the DICP discharge at the middle position. Power varied between 500, 750 and 1000 W. For all applied powers, pressure varied between 3, 6, 8 and 10 Pa. It can be seen that intensity increased with decreasing pressure. Also, at every pressure, higher power led to higher intensity. Lower pressure leads to notably higher electron temperatures, which leads to a higher excitation rate. Therefore, intensity is increased, despite a lower gas density at the lower pressure.

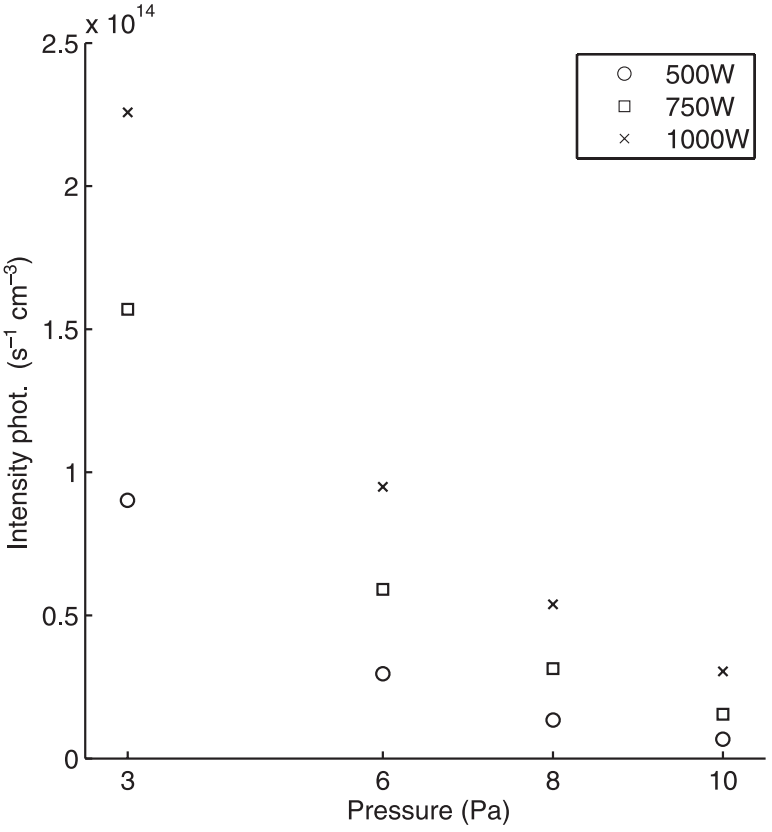

FIG. 8: Measured photon intensity at the middle position.

Fig. 9 shows calculated intensity values for pressure and power in the middle of the DICP reactor, which varied in a similar range as in the experiment. Similar to experimental values, lower pressure led to an increase in intensity; higher power also led to higher intensities. Calculated values show similar relative behavior as measured values; however, absolute values are offset from measured values. It can be observed that the offset is greatest for the lowest pressure and highest input power. At 3 Pa and 1000 W, the measured value is around 5 times higher than that in the simulation, whereas for 10 Pa and 1000 W, the measured value is twice the simulated value.

Results of spectroscopy and simulation are in good agreement in the active plasma zone. For the second measurement position in a remote area, it can be seen that simulated values were significantly lower, which were probably caused by the negligence of photon transport, stepwise excitation, and ionization of metastable hydrogen molecules.[36] Numerous metastable molecules, which have a long lifetime, are created in the active plasma zone and can diffuse throughout the plasma volume. Photons, which also are created in the active plasma zone, can then ionize

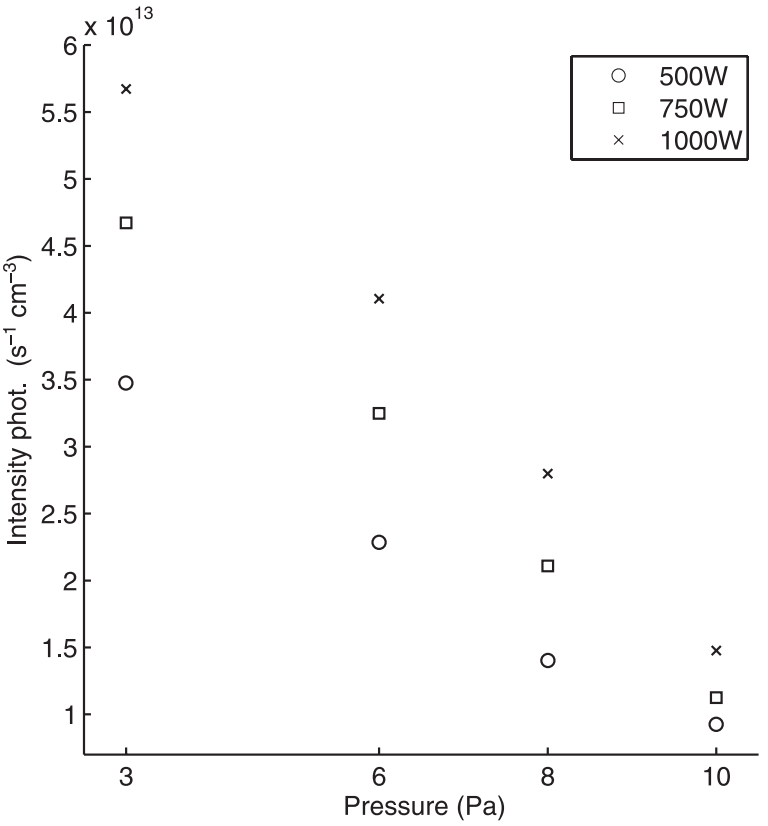

FIG. 9: Calculated photon intensity at the middle position.

metastable molecules in remote areas. The effect of this mechanism is pronounced in remote regions, and therefore simulation, which neglects this mechanism, gives a lower plasma density in remote areas. Further research has to be done to take this effect into account in order to achieve higher accuracy of simulation in remote areas of the discharge chamber.

Nevertheless, it can be seen that the simulated values are in good relative agreement with each other. It can be clearly seen that lower pressure leads to higher intensity; likewise does more power lead to higher intensity. Therefore, the prediction of radiation intensities should be feasible since relative accuracy is very high.

It is expected that a pressure exists that produces maximum intensity. Lower pressure leads to higher electron temperature, which exponentially contributes to intensity, as can be seen from corona model calculations. However, there exists a limit beyond which decreasing pressure will not lead to any further increase in radiation. Simulation of the active plasma zone shows this maximum between 3 and 6 Pa, and the measurement also hints to a maximum close to 3 Pa. Finding this value for every discharge is the ultimate goal when designing sterilization discharges. Furthermore, lower pressure

provokes better diffusion, which leads to a more uniform discharge. This is very helpful for sterilization purposes, since the complete surface of payload objects needs to be sterilized. It is preferably achieved by a homogeneous discharge.

IV. CONCLUSION

To get a better understanding of the interactions between plasma and the treated object, it is necessary to quantify UV irradiation. It has been shown that UV/VUV irradiation is a fast-acting sterilization method; furthermore, *A. brasiliensis* spores are not sterilized by UV radiation alone. Simulations are in good agreement with OES measurements, so plasma simulations can help to develop and optimize plasma discharges. Low-pressure plasma sterilization is ready for commercial use through its ability to sterilize endospores with a logarithmic reduction *R* greater than 6 inside a metal box with 0.3 mm slits (PCD); thus this is the worst location for plasma sterilization. DBD seems to be a good alternative for wound disinfection because it is capable of fast inactivation of *E. coli*.

REFERENCES

1. Kong MG, Kroesen G, Morll G, Nosenko T, Shimizu T, van Dijk J, Zimmerman JL. Plasma medicine: an introductory review. New J Phys. 2009;11(11):115012.
2. Lerouge S, Wertheimer M, Yahia LH. Plasma sterilization: a review of parameters, mechanisms, and limitations. Plasmas Polym. 2001;6(3):175–88.
3. Moisan M, Barbeau J, Moreau S, Pelletier J, Tabrizian M, Yahia LH. Low-temperature sterilization using gas plasmas: a review of the experiments and an analysis of the inactivation mechanisms. Int J Pharmaceut. 2001;226(1):1–21.
4. von Keudell A, Awakowicz P, Benedikt J, Raballand V, Yanguas-Gil A, Opretzka J, Flöttgen C, Reuter R, Byelykh L, Halfmann H, Staplemann K, Denis B, Winderlich J Muranyi P, Rossi F, Kylián O, Hasiwa N, Ruiz A, Rauscher H, Sirghi L, Comoy E, Dehen C, Challier L, Deslys JP. Inactivation of bacteria and biomolecules by low-pressure plasma discharges. Plasma Process Polym. 2010;7(3-4):327–52.
5. Stapelmann K, Kylian O, Denis B, Rossi F. On the application of inductively coupled plasma discharges sustained in Ar/O2/N2 ternary mixture for sterilization and decontamination of medical instruments. J Phys D Appl Phys. 2008;41(19):192005.
6. Rauscher H, Stapelmann K, Kylian O, Denis B, Rossi F. Monitoring plasma etching of biomolecules by imaging ellipsometry. Vacuum. 2009;84(1):75–8.
7. Kylian O, Denis B, Stapelmann K, Ruiz A, Rauscher H, Rossi F. Characterization of a low-pressure inductively coupled plasma discharge sustained in $Ar/O_2/N_2$ ternary mixtures and evaluation of its effect on erosion of biological samples. Plasma Process Polym. 2011;8(12):1137–45.
8. Kylian O, Rauscher H, Denis B, Ceriotti L, Rossi F. Elimination of homo-polypeptides of amino acids from surfaces by means of low-pressure inductively coupled plasma discharge. Plasma Process Polym. 2009;6(12):848–54.
9. Denis B, Steves S, Semmler E, Bibinov N, Novak W, Awakowicz P. Plasma sterilization of pharmaceutical products: from basics to production. Plasma Process Polym. 2012;9(6):619–29.

10. Kalghatgi SU, Fridman G, Cooper M, Nagaraj G, Peddinghaus M, Balasubramanian M, Vasilets VN, Gutsol AF, Fridman A, Friedman G. Mechanism of blood coagulation by nonthermal atmospheric pressure dielectric barrier discharge plasma. IEEE Trans Plasma Sci. 2007;35(5):1559–66.
11. Shekhter AB, Serezhenkov VA, Rudenko TG, Pekshev AV, Vanin AF. Benecial effect of gaseous nitric oxide on the healing of skin wounds. Nitric Oxide. 2005;12(4):210–9.
12. Fridman G, Peddinghaus M, Balasubramanian M, Ayan H, Fridman A, Gutsol A, Brooks A. Blood coagulation and living tissue sterilization by oating-electrode dielectric barrier discharge in air. Plasma Chem Plasma Process. 2006;26(4):425–42.
13. Vandamme M, Robert E, Dozias S, Sobilo J, Lerondel S, Le Pape A, Pouvesle JM. Response of human glioma U87 xenografted on mice to non thermal plasma treatment. Plasma Med. 2011;1(1):27–43.
14. Vandamme M, Robert E, Lerondel S, Sarron V, Ries D, Dozias S, Sobilo J, Gosset D, Kieda C, Legrain B, Pouvesle JM, Pope LA. ROS implication in a new antitumor strategy based on non-thermal plasma. Int J Cancer. 2011;130(9):2185–94.
15. Weltmann K, Brandenburg R, Von Woedtke T, Ehlbeck J, Foest R, Stieber M, Kindel E. Antimicrobial treatment of heat sensitive products by miniaturized atmospheric pressure plasma jets (APPJs). J Phys D Appl Phys. 2008;41(19):194008.
16. Dobrynin D, Wu A, Kalghatgi S, Park S, Shainsky N, Wasko K, Dumani E, Ownbey R, Joshi S, Sensenig R, Brooks AD. Live pig skin tissue and wound toxicity of cold plasma treatment. Plasma Med. 2011;1:93–108.
17. Schneider S, Lackmann JW, Ellerweg D, Denis B, Narberhaus F, Bandow JE, Benedikt J. The role of VUV radiation in the inactivation of bacteria with an atmospheric pressure plasma jet. Plasma Process Polym. 2012;9(6):561–8.
18. Schneider S, Lackmann JW, Narberhaus F, Bandow JE, Denis B, Benedikt J. Separation of VUV/UV photons and reactive particles in the euent of a He/O_2 atmospheric pressure plasma jet. J Phys D Appl Phys. 2011;44(29):295201.
19. Halfmann H, Bibinov N, Wunderlich J, Awakowicz P. A double inductively coupled plasma for sterilization of medical devices. J Phys D Appl Phys. 2007;40(14):4145.
20. Keller S, Rajasekaran P, Bibinov N, Awakowicz P. Characterization of transient discharges under atmospheric-pressure conditions applying nitrogen photoemission and current measurements. J Phys D Appl Phys. 2012;45(12):125202.
21. Rajasekaran P, Mertmann P, Bibinov N, Wandke D, Viöl W, Awakowicz P. Filamentary and homogeneous modes of dielectric barrier discharge (DBD) in air: investigation through plasma characterization and simulation of surface irradiation. Plasma Process Polym. 2010;7(8):665–75.
22. Rajasekaran P, Opländer C, Homeister D, Bibinov N, Suschek CV, Wandke D, Awakowicz P. Characterization of dielectric barrier discharge (DBD) on mouse and histological evaluation of the plasma-treated tissue. Plasma Process Polym. 2011;8(3):246–55.
23. Rajasekaran P, Ruhrmann C, Bibinov N, Awakowicz P. Space-resolved characterization of high frequency atmospheric-pressure plasma in nitrogen, applying optical emission spectroscopy and numerical simulation. J Phys D Appl Phys. 2011;44(48):485205.
24. Moeller R, Horneck G, Facius R, Stackebrandt E. Role of pigmentation in protecting Bacillus sp. endospores against environmental UV radiation. FEMS Microbiology Ecology. 2006;51(2):231–6.
25. Muranyi P, Wunderlich J, Heise M. Sterilization eciency of a cascaded dielectric barrier discharge. J Appl Microbio. 2007;103(5):1535–44.

26. Muranyi P, Wunderlich J, Heise M. In uence of relative gas humidity on the inactivation eciency of a low temperature gas plasma. J Appl Microbio. 2008;104(6):1659–66.
27. Muranyi P, Wunderlich J, Langowski HC. Modication of bacterial structures by a low-temperature gas plasma and in uence on packaging material. J Appl Microbio. 2010;109(6):1875–85.
28. Bibinov N, Halfmann H, Awakowicz P, Wiesemann K. Relative and absolute intensity calibrations of a modern broadband echelle spectrometer. Meas Sci Technol. 2007;18(5):1327.
29. Bibinov N, Bolshukhin D, Kokh D, Pravilov A, Vinogradov I, Wiesemann K. Absolute calibration of the eciency of a VUV-monochromator/detector system in the range 110-450 nm. Meas Sci Technol. 1999;8(7):773.
30. Bibinov N, Kokh D, Kolokolov N, Kostenko V, Meyer D, Vinogradov IP, Wiesemann K. A comparative study of the electron distribution function in the positive columns in N_2 and N_2/H_e dc glow discharges by optical spectroscopy and probes. Plasma Sources Sci Technol. 1999;7(3):298.
31. Steves S, Ozkaya B, Liu CN, Ozcan O, Bibinov N, Grundmeier G, Awakowicz P. Silicon oxide barrier lms deposited on PET foils in pulsed plasmas: in uence of substrate bias on deposition process and lm properties. J Phys D Appl Phys. 2013;46(8):084013.
32. Bibinov N, Rajasekaran P, Mertmann P, Wandke D, Viol W, Awakowicz P. Basics and biomedical applications of dielectric barrier discharge (DBD). In: Laskovski AN, editor. Biomedical engineering, trends in materials science. Rijeka, Croatia: InTech; 2011. p.123–50.
33. Kushner MJ. Hybrid modelling of low temperature plasmas for fundamental investigations and equipment design. J Phys D Appl Phys. 2009;42(19):194013.
34. Halfmann H, Denis B, Bibinov N, Wunderlich J, Awakowicz P. Identication of the most ecient VUV/UV radiation for plasma based inactivation of Bacillus atrophaeus spores. J Phys D Appl Phys. 2007;40(19):5907.
35. Vicoveanu D, Popescu S, Ohtsu Y, Fujita H. Competing inactivation agents for bacterial spores in radio-frequency oxygen plasmas. Plasma Process Polym. 2008;5(4):350–58.
36. Lichten W. Metastable hydrogen molecules. Phys Rev. 1960;120(3):848–53.